

# Low-threshold surface-passivated photonic crystal nanocavity laser

Dirk Englund<sup>a)</sup>

Department of Applied Physics, Stanford University, Stanford, California 94305

Hatice Altug

Electrical and Computer Engineering Department, Boston University, Boston, Massachusetts 02215

Jelena Vučković

Ginzton Laboratory, Stanford University, Stanford, California 94305

(Received 22 March 2007; accepted 19 July 2007; published online 17 August 2007)

The efficiency and operating range of a photonic crystal laser are improved by passivating the In-GaAs quantum well gain medium and GaAs membrane using a (NH<sub>4</sub>)S treatment. The passivated laser shows a fourfold reduction in nonradiative surface recombination rate, resulting in a fourfold reduction in lasing threshold. A three-level carrier dynamics model explains the results and shows that typical parameters of such lasers lead to a lasing threshold as much determined by surface recombination as by the overall impact of the cavity quality factor. Surface passivation therefore appears crucial in operating such lasers under practical conditions. © 2007 American Institute of Physics. [DOI: 10.1063/1.2769957]

Photonic crystals (PCs) allow unprecedented control over the radiative properties of integrated emitters. By defining small mode-volume, high-quality factor ( $Q$ ) cavities in PCs, enhanced light-matter interaction becomes possible. This property has opened possibilities in fields including cavity quantum electrodynamics, detection, and light sources. Lasers, in particular, stand to gain through dramatically improved lasing threshold, modulation rate, cost, and large-scale device integration. From their first demonstration,<sup>1</sup> PC lasers have most commonly relied on quantum wells (QWs) for optical gain. However, QWs limit PC laser performance in many material systems because of large nonradiative (NR) surface recombination. This problem is particularly damaging in PC structures where embedded QWs expose a large surface area. Here we address the NR recombination problem by surface passivation. We show that (NH<sub>4</sub>)S-mediated surface passivation of PC laser structures lowers the NR recombination rate by more than four times and leads to a fourfold reduction of lasing threshold. The increased efficiency extends the operating range from cryogenic to practical regimes, enabling room-temperature lasing at terahertz-modulation rates, as described in Ref. 2. A three-level rate equation model fits our experimental data well and suggests that surface passivation is crucial for PC lasers in InGaAs/GaAs and other material systems with fast NR surface recombination.

The PC nanocavity lasers consist of 172-nm-thick GaAs slabs patterned with  $9 \times 9$  arrays of single-hole cavities defined in a square-lattice PC, similar to those described in Ref. 3. A central stack of four 8 nm In<sub>0.2</sub>Ga<sub>0.8</sub>As QWs, spaced by 8 nm GaAs barriers, forms the gain medium.

This sample is passivated using a solution of 7% (NH<sub>4</sub>)S in water. The treatment removes contamination and oxides from the GaAs and In<sub>0.2</sub>Ga<sub>0.8</sub>As surfaces and caps the fresh surface with sulfur atoms.<sup>4</sup> Samples were first cleaned in Leksol, acetone, and ethanol, then submerged in the (NH<sub>4</sub>)S solution for 15 min at 35 °C, and finally air-dried, following

Ref. 5. We measured the radiative and NR properties, as well as lasing characteristics, before and after surface passivation.

Before presenting the experimental results, we describe the carrier dynamics at low temperature ( $\sim 10$  K) using a three-level rate model. Letting  $N_E$  represent the pump-level carrier concentration (populated above the GaAs band gap using a laser with power  $L_{in}$ ),  $N_G$  the QW lasing level carrier concentration (resonant with the cavity frequency), and  $P$  the coupled cavity photon density, we have<sup>6</sup>

$$\begin{aligned} \frac{dP}{dt} &= \Gamma G(N_G)P + \frac{F_{cav}N_G}{\tau_r} - \frac{P}{\tau_p}, \\ \frac{dN_G}{dt} &= \frac{N_E}{\tau_{E,f}} - N_G \left( \frac{F_{cav} + F_{PC}}{\tau_r} + \frac{1}{\tau_{PC,nr}} \right) - \Gamma G(N_G)P, \\ \frac{dN_E}{dt} &= \eta \frac{L_{in}}{\hbar \omega_p V_a} - N_E \left( \frac{1}{\tau_{E,r}} + \frac{1}{\tau_{E,nr}} + \frac{1}{\tau_{E,f}} \right). \end{aligned} \quad (1)$$

In the top equation, the cavity photon density is driven by the QW through stimulated emission (first term) and spontaneous emission (SE) at the Purcell-enhanced rate  $F_{cav}/\tau_r$ , while losing photons at the cavity loss rate  $1/\tau_p$ . The lasing level concentration  $N_G$  in the center equation is pumped by carrier relaxation from the pump level  $N_E$  at rate  $\tau_{E,f}$ . Besides pumping the cavity,  $N_G$  decays through NR channels at rate  $1/\tau_{PC,nr}$  and PC leaky modes at rate  $F_{PC}/\tau_r$ , where  $F_{PC} \approx 0.2$  expresses SE rate quenching inside the PC band gap compared to the SE rate  $1/\tau_r$  in the bulk QW (following simulations in Ref. 7). In the bottom equation, the  $N_E$  level is pumped through above-band optical excitation with power  $L_{in}$  (the first term) and decays through carrier relaxation into  $N_G$ , NR recombination, and SE (second term).

We estimate the lifetime constants in Eq. (1) from time-resolved photoluminescence (PL) recorded with a streak camera (Hamamatsu N5716-03) in the confocal microscope setup shown in Ref. 8. The measurements are performed separately on PC mirrors and bulk regions with 3.5 ps long excitation pulses at 780 nm wavelength and 82 MHz repetition rate [Figs. 1(b) and 1(c)]. The strong effect of NR re-

<sup>a)</sup>Electronic mail: englund@stanford.edu.

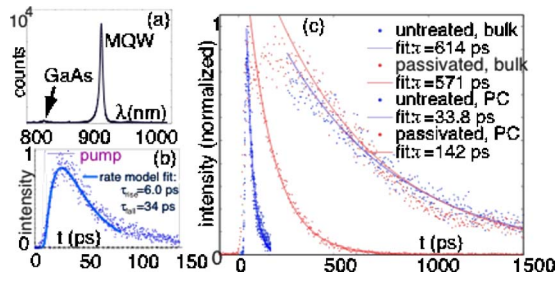


FIG. 1. (Color online) Low-temperature photoluminescence measurements on unpatterned and PC regions. (a) PL from the bulk sample (after passivation). (b) Expanded view of PL from untreated PC region shows short lifetime  $\tau_{PC} \approx 33.8$  ps; the data are fitted by the rate model of Eq. (1). (c) PL measurements for the untreated (blue) and passivated (red) samples, from the PC and unpatterned regions.

combination is evident in the far shorter lifetime in the PC region. Samples were cooled to 10 K in a liquid-helium continuous-flow cryostat so that both unpassivated and passivated samples could be brought into lasing for comparison. From a fit of Eq. (1) to the rise time of PL from the untreated sample, shown in Fig. 1(b), we estimate the relaxation time from the pump level into the lasing level at  $\tau_{E,f} \sim 6$  ps. The passivated sample also gives  $\tau_{E,f} \sim 6$  ps.

Figure 1(c) shows the reduction in NR surface recombination after passivation: the PL decay lifetime from the PC mirror region is extended to  $\tau_{PC} \sim 142$  ps from  $\tau_{PC} \sim 33.8$  ps before passivation, while the decay lifetime from the bulk QW has nearly unchanged lifetime  $\tau_{bulk} \sim 571$ – $614$  ps at  $10 \mu\text{W}$  pump power. These data are analyzed using the bottom two equations of Eq. (1) applied to PC and bulk regions, i.e.,  $1/\tau_i = 1/\tau_{i,nr} + F_i/\tau_r$  with  $i$  denoting bulk or PC ( $F_{bulk} = 1$ ). Assuming the carrier recombination in the bulk semiconductor is dominantly radiative, the lifetime data then let us estimate the unpatterned bulk SE lifetime  $\tau_r \approx 654$  (605) ps and NR lifetime  $\tau_{PC,nr} \approx 35.5$  (149) ps in the PC mirrors before (after) passivation. We assume equal NR lifetime across the cavity and surrounding PC mirrors since the diffusion length of rate-limiting holes is  $\sim 3 \mu\text{m}$ , greatly exceeding the cavity size.

To put this reduction in NR loss rate into perspective and compare it to reports on other types of structures, we extract the surface recombination velocity  $S$  that describes the recombination at the QW surface. From the lifetime data in Fig. 1(c), it is clear that most NR recombination results from the PC holes. The effect of passivation is therefore to reduce  $S$ , and a simple model allows us to quantify by how much (pump power is small enough to neglect Auger recombination). The diffusion and recombination of the QW carrier concentration  $N_G$ , uncoupled to the PC cavities, are described by the equation (following Ref. 9)

$$\frac{\partial N_G}{\partial t} = D \nabla^2 N_G - N_G \frac{F_{PC}}{\tau_r}, \quad (2)$$

where  $D$  is the ambipolar diffusion coefficient. Surface recombination enters through the boundary condition  $D(\partial N_G / \partial r) + S N_G = 0$  at the hole walls. Assuming isotropic minority-carrier density over the PC period  $a = 315$  nm, the total recombination rate of the PC depends only on the exposed QW surface area. This area is equal if the PC is replaced with an array of mesas whose radius equals the PC hole radius  $r$ . Equation (2) is then easily solved in cylindrical coordinates,<sup>9</sup> giving the total recombination rate  $1/\tau_{PC}$

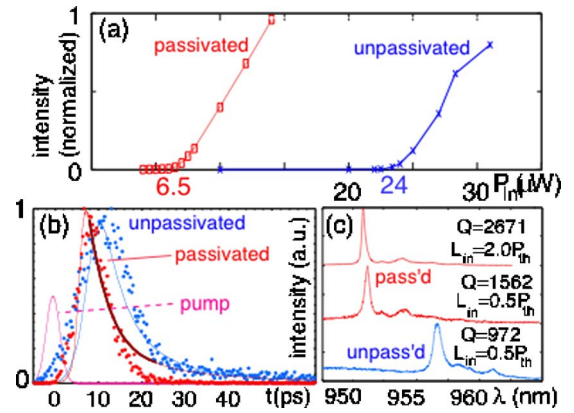


FIG. 2. (Color online) Cavity resonances below and above lasing threshold. (a) Lasing curves for unpassivated and passivated structures at low temperature (10 K) with pulsed excitation (3.5 ps, 13 ns repetition). Passivation reduces threshold from 24 to  $6 \mu\text{W}$  averaged power (measured before an objective lens focusing to an  $\sim 3 \mu\text{m}$  radius spot). (b) Laser time response for untreated (blue) and treated (red) samples at 10 K; Eq. (1) fits the data well. The treated laser shows an exponential decay time of 6.1 ps (thick fit). Some deviations at longer times are caused by background PL from regions not coupled to the resonant mode. (c) Cavity resonances below and above lasing. Passivation lowers the resonance wavelength and slightly increases  $Q$ , as seen in the untreated (blue) and treated (red) cavity spectra at  $1/2$  threshold pump power. Top spectrum (red): lasing of passivated structure, pumped two times above threshold.

$= F_{PC}/\tau_r + 1/\tau_{PC,nr} = F_{PC}/\tau_r + 2S/r$ , i.e.,  $\tau_{PC,nr} = r/2S$ . We then find that  $S \approx 1.7 \times 10^5$  cm/s ( $4.0 \times 10^4$  cm/s) for the original (passivated) structure. This value for the surface recombination velocity is somewhat lower than previous room-temperature measurements on similar InGaAs/GaAs structures by Refs. 10 and 11, which put it at between  $\sim 1 \times 10^5$  and  $5 \times 10^6$  cm/s. This is expected, since  $S \propto v_{th} \approx \sqrt{3kT/m^*}$ , the thermal velocity, which is approximately five times smaller at 10 K.<sup>12</sup> Our observation of a fourfold lowering in  $S$  with surface passivation is similar to other reports with  $(\text{NH}_4)\text{S}$ .<sup>13</sup> However, better passivation results could probably be achieved with  $(\text{NH}_4)\text{S}_x$ ,  $x > 1$ , for which up to 50 times improvement was reported.<sup>10</sup>

With this understanding of the carrier dynamics in the PC, we now consider the coupled cavity array laser. Microscope images show that only seven to nine cavities simultaneously lase in a single mode as fabrication inaccuracies lifted the cavity array's resonance degeneracies. Figure 2(c) shows that the passivation treatment slightly blueshifts the cavity resonance and raises  $Q$  by  $\sim 1.5$  times by cleaning and thinning the membrane, as observed in digital cavity etching.<sup>14</sup> The figure also shows the passivated structure when pumped two times above threshold;  $Q$  is then raised to 2670 due to gain. We estimate the average SE enhancement factor  $F_{cav}$  of emission coupled to the PC cavities from a lifetime measurement of the nonlasing cavity measured at  $\sim 1/2$  lasing threshold, giving  $\tau_{cav} \approx 17$  ps. The relation for the cavity-coupled SE rate,

$$\frac{1}{\tau_{cav}} = \frac{F_{cav} + F_{PC}}{\tau_r} + \frac{1}{\tau_{PC,nr}}, \quad (3)$$

gives  $F_{cav} \approx 33$ .

Figure 2(a) shows the lasing curves for the original and passivated structures and indicates a fourfold reduction in the threshold pump power  $L_{in,th}$ . To approximate the threshold reduction in a simple analytical model, we consider the

steady-state lasing threshold. Although this is not completely appropriate for the short pulses considered here, numerical simulations show that the steady-state threshold approximation explains the effect of nonradiative recombination in our system well. We solve Eq. (1) at threshold, defined here at the power  $PV_{\text{mode}}=1$  (corresponding to equal stimulated and spontaneous emission rates).<sup>15</sup> Neglecting the slow pump-level radiative recombination  $\tau_{E,r}$ , this gives

$$L_{\text{in,th}} = \frac{\hbar\omega_p V_a}{\tau_p \eta V_{\text{mode}}} \left[ N_{\text{th}} V_{\text{mode}} \left( F_{\text{PC}} \frac{\tau_p}{\tau_r} + \frac{\tau_p}{\tau_{\text{PC,nr}}} \right) + 1 \right] \left( 1 + \frac{\tau_{E,f}}{\tau_{E,nr}} \right). \quad (4)$$

For typical parameters, we find that the threshold carrier density roughly equals the transparency carrier density  $N_{\text{tr}} \approx 10^{18} \text{ cm}^{-3}$  (Ref. 16) and  $V_{\text{mode}} \approx 6(\lambda/n)^3$ , the first term in the brackets dominates. Within this term, the nonradiative part  $\tau_p/\tau_{\text{nr}}$  dominates the radiative one  $F_{\text{PC}}\tau_p/\tau_r$ . Thus, in PC lasers using InGaAs QWs, or other gain media with similar surface recombination velocity, threshold is largely determined by NR recombination losses at the QW and GaAs membrane surfaces. After passivation, Eq. (4) predicts a threshold reduction by a factor of 4.1 of the original value if the NR pump-level loss rate  $1/\tau_{E,nr}$  is assumed to be much smaller than the relaxation rate  $1/\tau_{E,f}$  into the lasing level (otherwise an even larger reduction). We measured a decrease by a factor of 3.7, which shows good agreement with the predicted value. The differential quantum efficiency, on the other hand, is nearly unaffected by the NR recombination rate, as can be easily derived from the rate equations (the physical reason is that once lasing begins, the stimulated emission rate is much faster than the NR loss rate).

One of the most remarkable aspects of the PC nanocavity laser is the extremely fast modulation rate. In Fig. 2(b), we present streak camera measurements of the lasing response to 3.4 ps long pump pulses. The low-temperature measurements for the passivated and unpassivated samples were obtained at the same average pump power of  $\sim 28 \mu\text{W}$  (3.5 ps, 13 ns repetition), and the normalized lasing response is compared in the red and blue plots. After passivation, the laser responds somewhat faster with an exponential decay time of 6.1 ps. We attribute this speed up largely to relatively higher pump power above threshold due to lower NR loss and higher cavity  $Q$  (which results in Purcell-enhanced spontaneous emission and slightly decreased threshold in pulsed response). Faster time response is possible at higher pump power, as noted in Ref. 3. The rate model of Eq. (1) explains these time-response measurements well, as shown in the continuous-line fits.

In conclusion, we have demonstrated the threshold-lowering effect of surface-passivation treatment of InGaAs QWs in a PC coupled nanocavity array laser. The four-fold

reduction of NR surface recombination lowers the threshold pump power to 27% of its original value. Our three-level laser model agrees well with the experimental observations and shows that NR recombination strongly affects lasing when the NR loss rate is faster than the modified SE rate in the PC. In this regime, the steady-state threshold approximation Eq. (4) indicates that threshold is in large part dictated by material parameters  $N_{\text{th}}$ ,  $V_a$ , and  $\tau_{\text{nr}}$ . Using a carrier diffusion model, we calculate a drop in the QW surface recombination velocity from  $S \approx 1.7 \times 10^5$  to  $3.2 \times 10^4 \text{ cm/s}$  after passivation; comparing this to literature, we believe that our results could be improved by applying better surface-passivation techniques.<sup>10,17</sup> The increased efficiency achieved in our lasers alleviates heating problems, which opens the door to room-temperature and cw operation<sup>2</sup> and brings PC lasers closer to practical applications.

The authors thank D. Y. Petrovykh for his helpful comments. This work was supported by the MARCO IFC Center, NSF Grant Nos. ECS-0424080 and ECS-0421483, the MURI Center (ARO/DTO Program No. DAAD19-03-1-0199), as well as the NDSEG Fellowship to one of the authors (D.E.).

<sup>1</sup>O. Painter, R. Lee, A. Scherer, A. Yariv, J. O'Brien, P. Dapkus, and I. Kim, *Science* **284**, 1819 (1999).

<sup>2</sup>D. Englund, H. Altug, and J. Vuckovic, *Appl. Phys. Lett.* **91**, 071126 (2007).

<sup>3</sup>H. Altug, D. Englund, and J. Vučković, *Nat. Phys.* **2**, 484 (2006).

<sup>4</sup>H. Oigawa, J. F. Fan, Y. Nannichi, H. Sugahara, and M. Oshima, *Jpn. J. Appl. Phys., Part 1* **30**, 322 (1991).

<sup>5</sup>D. Y. Petrovykh, M. Yang, and L. Whitman, *Surf. Sci.* **523**, 231 (2002).

<sup>6</sup> $V_a$  is the pump active volume,  $\omega_p$  is the cavity angular frequency,  $\tau_p = Q/\omega_p$  is the cavity ring-down time,  $G(N)$ , is the gain;  $\Gamma \approx 0.16$  is the gain confinement factor for cavity mode with four 8 nm QWs,  $\eta$  is the pump power absorption ratio,  $\tau_r$  is the SE lifetime in unpatterned QW,  $\tau_{\text{PC,nr}}$  is the NR lifetime in PC, and  $\tau_{E,f}$ ,  $\tau_{E,r}$ , and  $\tau_{E,nr}$  are the lifetimes of pump-level relaxation, SE, and NR transitions.

<sup>7</sup>D. Englund, D. Fattal, E. Waks, G. Solomon, B. Zhang, T. Nakaoka, Y. Arakawa, Y. Yamamoto, and J. Vučković, *Phys. Rev. Lett.* **95**, 013904 (2005).

<sup>8</sup>D. Englund, A. Faraon, B. Zhang, Y. Yamamoto, and J. Vuckovic, *Opt. Express* **15**, 5550 (2007).

<sup>9</sup>K. Tai, T. R. Hayes, S. L. McCall, and W. T. Tsang, *Appl. Phys. Lett.* **53**, 302 (1988).

<sup>10</sup>G. Beister and H. Wenzel, *Semicond. Sci. Technol.* **19**, 494 (2004).

<sup>11</sup>S. Y. Hu, S. W. Corzine, K.-K. Law, D. B. Young, A. C. Gossard, and L. A. Coldren, *J. Appl. Phys.* **76**, 4479 (1994).

<sup>12</sup>S. M. Sze, *Physics of Semiconductor Devices*, 2nd ed. (Wiley-Interscience, New York, 1981), p. 57.

<sup>13</sup>M. Boroditsky, I. Gontijo, M. Jackson, R. Vrijen, E. Yablonovitch, T. Krauss, C.-C. Cheng, A. Scherer, R. Bhat, and M. Krames, *J. Appl. Phys.* **87**, 3497 (2000).

<sup>14</sup>K. Hennessy, A. Badolato, A. Tamboli, P. Petroff, E. Hu, M. Atature, J. Dreiser, and A. Imamoglu, *Appl. Phys. Lett.* **87**, 021108 (2005).

<sup>15</sup>G. Björk and Y. Yamamoto, *IEEE J. Quantum Electron.* **27**, 2386 (1991).

<sup>16</sup>L. A. Coldren and S. W. Corzine, *Diode Lasers and Photonic Integrated Circuits* (Wiley, New York, 1995), Chap. 4.

<sup>17</sup>D. Y. Petrovykh, J. P. Long, and L. J. Whitman, *Appl. Phys. Lett.* **86**, 242105 (2005).